Structure Characterization and Immunomodulating Effects of Polysaccharides Isolated from Dendrobium officinale

Wei, Wei; Feng, Lei; Bao, Wan-Rong; Ma, Dik-Lung; Leung, Chung-Hang; Nie, Shao-Ping; Han, Quan-Bin

Published in:
Journal of Agricultural and Food Chemistry

DOI:
10.1021/acs.jafc.5b05180

Published: 01/02/2016

Document Version:
Peer reviewed version

Structure characterization and immunomodulating effects of polysaccharides isolated from *Dendrobium officinale*

Wei Wei[a]*, Lei Feng[a,b]*, Wan-Rong Bao[a], Dik-Lung Ma[c], Chung-Hang Leung[d], Shao-Ping Nie [b]**, Quan-Bin Han[a]**

[a]*School of Chinese Medicine, Hong Kong Baptist University, Hong Kong, China*
[b] *State Key Laboratory of Food Science and Technology, Nanchang University, Nanchang, Jiangxi, China;*
[c]*State Key Laboratory of Quality Research in Chinese Medicine, Institute of Chinese Medical Sciences, University of Macau, Macao, China;*
[d]*Department of Chemistry, Hong Kong Baptist University, Hong Kong, China*

*Equal contribution

**Corresponding authors:

Q.B. Han
7 Baptist University Road, School of Chinese Medicine, Hong Kong Baptist University, Kowloon Tong, Hong Kong SAR, China
Tel: 00852-34112906 / Fax: 00852-34112461
E-mail: simonhan@hkbu.edu.hk

S.P. Nie
State Key Laboratory of Food Science and Technology, Nanchang University, Nanchang, Jiangxi, China
Tel/Fax: 0086-791-88304452
E-mail: spnie@ncu.edu.cn …

Abstract

A crude polysaccharide fraction (cDOP) has been determined to be the characteristic marker of *Dendrobium officinale*, an expensive tea material in Asia, but its chemistry and bioactivity have not been studied. In work reported here, cDOP was de-starched (DOP, 90% yield), and separated into two polysaccharides, DOP-1 and DOP-2, which were characterized by monosaccharide composition and methylation analyses, and spectral analyses (FT-IR and ^{1}H and ^{13}C NMR). Both are composed of mannose and glucose, at similar ratios; and have a similar structure with a backbone of 1,4-linked β-$_{D}$-mannopyranosyl and β-$_{D}$-glucopyranosyl residues. Significant differences were observed only in their molecular weights. Bioassay using mouse macrophage cell line RAW 264.7 indicated that DOP and its two sub-fractions enhance cell proliferation, TNF-α secretion, and phagocytosis in a dose-dependent manner. They also induced the proliferation of lymphocytes alone and with mitogens. DOP-1 and DOP-2 are thus proven to be major, active polysaccharide markers of *D. officinale*.

Keywords: *Dendrobium officinale*, polysaccharides, chemical structure, RAW264.7 cells, lymphocytes

1. Introduction

Dendrobium is one of the largest genera in the plant family Orchidaceae. More than 1100 species of *Dendrobium* have been identified, with a wide distribution throughout Asia, Europe and Australia (*1*). Totally, 74 species are found in China and more than 50 of them can be used as "*Shihu*", a well-known and expensive China tea. Dendrobii Officinalis Caulis, called *Tiepi Shihu* in Chinese, which is derived from dried stems of *Dendrobium officinale* Kimura et Migo, is traditionally recognized as the best *Dendrobium* species for tonic purposes, such as benefiting the stomach, supplementing body fluids and strengthening immunity (*2, 3*). In addition, its green stem can be either chewed directly or stewed in porridge, soup and dishes as a high-quality food in diets (*4*). More and more companies tend to use *D. officinale* stem as dietary supplements to develop functional beverages (*5*).

For selling in herbal markets, the stems of *D. officinale* are always heated, twisted into a spiral or spring form, and finally dried; in this form, it is commonly known as *Tiepi Fengdou*. Nowadays, due to extremely scarce wild resources and increasing demand, *Tiepi Fengdou* has become one of the most expensive tea materials in herb markets worldwide, particularly in Southeast Asia. The high diversity of species in the *Dendrobium* genus, a lack of distinguishing macroscopic identifying characteristics, and high price of *Tiepi Fengdou* have led to the occurrence of adulterants, confused species, and counterfeits (*6*). Authentication of *Tiepi Fengdou* has been a challenge for a long time. A reliable, accurate means of identifying

63 true *Tiepi Fengdou* would bring clarity to an uncertain market, allowing authorities to
64 regulate and certify the authentic species, giving consumers confidence, and safeguarding the
65 reputation of this expensive China tea.

66 Continous efforts have been made for authentication of *D. officinale* (*2*). Different
67 methods, like microscopic identification, DNA barcoding, fingerprinting small molecules,
68 and fingerprinting monosaccharide composition, have been studied but all have significant
69 weaknesses. Neither microscopic identification nor DNA barcoding is easy, and both need
70 well-trained hands to operate the instruments. More importantly, neither of them can present
71 quantitative analysis and therefore they will not work if the sample is true but its chemicals
72 have been extracted. Fingerprinting of both small molecules and hydrolysis products of
73 polysaccharide (monosaccharide composition) has also been studied (*7-11*); however, these
74 methods cannot reliably distinguish *Teipi Shihu* from other *Dendrobium* species**.**

75 In our previous study, we collected authentic *Teipi Shihu* samples from 5 GAP farms
76 (mainly in Yunnan Province), 10 other *Dendrobium* species, and 13 commercial samples
77 from HK local herb stores; and compared their molecular size distribution patterns using
78 HPLC coupled with HPGPC (high-performance gel permeation chromatography). Excitingly,
79 the authentic samples from GAP farms displayed identical and unique HPGPC profiles with a
80 huge peak (named cDOP) with molecular size in the range of 276-877 kDa. This peak was
81 selected as the authentication marker, because it has not been found in other *Dendrobium*

82 species. This marker has been successfully used as a QC marker in qualitative and
83 quantitative analysis of *Dendrobium* samples using HPGPC methods; however, little is
84 known about its chemical structure and bioactivity.

85 In this study, we report the isolation and purification of two water soluble linear
86 glucomannans (DOP-1 and DOP-2) from this QC marker. We have characterized their
87 chemical structures using monosaccharide composition analysis, methylation analysis, and
88 spectral analysis of their FT-IR, ESI-MS, GC–MS, and NMR spectra. Their effects on murine
89 macrophage RAW 264.7 cells and murine lymphocytes were also assayed.

90 ## 2. Materials and methods

91 ### *2.1. Materials*

92 The authentic *Dendrobium officinale* sample, also named *Tiepi Fengdou*, was kindly
93 provided by certified production area in mainland China and authenticated by Dr. Chen
94 Hubiao (*12*). A voucher specimen was deposited at the School of Chinese Medicine in Hong
95 Kong Baptist University, Hong Kong.

96 Monosaccharide standards for D-mannose (Man) and D-glucose (Glc) were purchased
97 from Merck Co. (Darmstadt, Germany). Thermostable α-amylase (29,559 units/mL),
98 iodomethane, sodium borohydride, sodium borodeuteride (98% atom% D), and dextran
99 standards with different molecular weights (M_W. 1.1×10^6, 6.7×10^5, 4.1×10^5, 2.7×10^5, 1.5×10^5,

100 8.0×10^4, 2.5×10^4, and 1.2×10^4 Da) were all purchased from Sigma-Aldrich (St. Louis, MO,
101 USA). Deuterium oxide (99.9% D) was purchased from J&K Scientific Ltd (Beijing, China).
102 A total starch assay kit (K-TSTA) was obtained from Megazyme (Wicklow, Ireland). All the
103 other chemicals or solvents were of analytical grade. Ultrapure water was produced by
104 Milli-Q system (Millipore, Billerica, USA).

105 LPS (from *Escherichia coli* 0111:B4), Griess reagent (modified), Concanavalin A (Con
106 A), polymyxin B sulfate salt (poly B), and
107 3-(4,5-dimethylthiazol-2-yl)-2,5-diphenyltetrazolium bromide (MTT) were purchased from
108 Sigma-Aldrich (St. Louis, MO, USA). Mouse IL-6 and TNF-α ELISA kits were purchased
109 from eBioscience (San Diego, CA, USA). The kit (CellTiter 96® AQueous One Solution Cell
110 Proliferation Assay) was purchased from Promega Inc. (Madison, WI, USA).

111 Animals: Inbred strain female (6 to 8 week-old) BALB/c mice were purchased from the
112 Laboratory Animal Services Centre of The University of Hong Kong. The animals were
113 provided with standard pellet diet and water ad libitum and maintained under controlled
114 conditions of temperature and humidity, with a 12 h light/dark cycles. All experiments with
115 animals were carried out in accordance with the Animals Ordinance, Department of Health,
116 Hong Kong Special Administration Region, China for the care and use of experimental
117 animals. All of the experimental protocols were first approved by the Committee on Use of
118 Human and Animal Subjects in Teaching and Research of the Hong Kong Baptist University.

119 *2.2. Extraction and purification of polysaccharides from D. officinale*

120 The dried powder of *Dendrobium officinale* (200 g) was defatted with 95% ethanol for 2
121 days at room temperature under stirring. After filtration, the residue was treated twice with 2
122 L ultrapure water at 100 ºC for 2 h and filtered. The combined extracts were centrifuged
123 (8,000 rpm, 10 min), and concentrated in a rotary evaporator under reduced pressure at 55 ºC.
124 Then the gel-like solution was precipitated by adding 3 volumes of 95% ethanol under
125 vigorous stirring. After standing overnight at 4 ºC, the precipitate was obtained by
126 centrifugation (8,000 rpm, 10 min), and further washed with absolute ethanol, acetone and
127 ether. Finally, the precipitate was dissolved in water, dialyzed against ultrapure water for 3
128 days, concentrated and lyophilized to yield the crude polysaccharide (cDOP).

129 Then, cDOP was de-starched according to Xing's method (*13*), and the obtained purified
130 *Dendrobium officinale* polysaccharide was designated as DOP. A total of 100 mg of DOP was
131 dissolved in 10 mL of ultrapure water and loaded onto a DEAE-650M anion-exchange
132 chromatography column (5.0 i.d. × 30 cm). The column was eluted with ultrapure water first
133 and then with 0.01, 0.03, 0.05, 0.10, and 0.30 M NaCl solutions at the flow rate of 1.5
134 mL/min. Fractions (20 mL) were collected by a fraction collector and the carbohydrate
135 content was analyzed by the phenol-sulphuric acid assay method (*14*). Two fractions, namely
136 DOP-1 (eluted by ultrapure water) and DOP-2 (eluted by 0.01 M NaCl), were successfully
137 separated from DOP, dialyzed for 48 h, concentrated and lyophilized.

138 *2.3. Structure analysis*

139 *2.3.1. Molecular weight determination*

140 Homogeneity and the molecular mass of DOP, DOP-1, and DOP-2 were determined
141 using high-performance gel-permeation chromatography (HPGPC) according to the method
142 of Xu (*12*). The analyses were performed on an Agilent 1100 series HPLC-DAD system
143 (Agilent Technologies, Palo Alto, CA, USA) coupled with evaporative light scattering
144 detector (ELSD, Grace, Deerfield, USA). Dextran standards with different molecular weights
145 (M_W: 1.1×10^6, 6.7×10^5, 4.1×10^5, 2.7×10^5, 1.5×10^5, 8.0×10^4, 2.5×10^4, and 1.2×10^4 Da) were
146 used for the calibration curve.

147 *2.3.2. Chemical components and monosaccharide composition*

148 The total sugar content was measured by phenol-sulphuric acid spectrophotometric
149 assay (*15*) and D-mannose was used as equivalents. The content of uronic acid was
150 determined by the modified carbazole and sulphuric acid method (*16*) with D-glucuronic acid
151 as the standard. Protein content was determined by spectrophotometric method (*17*) using
152 bovine serum albumin (BSA) as the standard. For monosaccharide composition analysis,
153 samples (5 mg) were hydrolyzed with 2 mL of 2 M trifluoroacetic acid (TFA) at 120 ºC for 2
154 h. Then, the resulting samples were analyzed using high-performance liquid chromatography
155 (HPLC) coupled with ELSD detector according to the method of Yang (*18*) with some

156 modifications. Instead of the gradient elution, an isocratic mobile phase consisting of 22:78
157 (v/v) mixtures of water and ACN was used.

158 *2.3.3. Infrared spectroscopic analysis of polysaccharides*

159 DOP and its two fractions (DOP-1 and DOP-2) were characterized by FT-IR
160 spectroscopy on a Thermo Nicolet 5700 infrared spectrophotometer (Thermo Electron,
161 Madison, WI, USA) at room temperature (25 ºC) using KBr pellets. Samples were dried at 55
162 ºC in a vacuum drying oven for 24 h prior to analysis, and spectra were scanned between
163 4000 cm^{-1} to 450 cm^{-1} with the resolution of 4 cm^{-1}.

164 *2.3.4 Methylation and GC-MS analysis*

165 The methylation analysis of DOP, DOP-1, and DOP-2 were carried out according to the
166 method of Carre (*19*) with some modifications (*20, 21*). Briefly, the dried samples were
167 dissolved in anhydrous DMSO with constant stirring at 50 ºC for 20 h to obtain a well
168 dissolved solution. Then, dry NaOH powder (20 mg) was added, and the mixture was stirred
169 at room temperature for 4 h. After that, methyl iodide (1.0 mL) was added slowly, with the
170 mixture in an ice bath, and another 0.5 mL methyl iodide was added 30 min later. The
171 solution was stirred for 2.5 h. The methylated polysaccharides were extracted with CH_2Cl_2,
172 and then washed with distilled water three times. In order to remove water, the extract was
173 passed through an anhydrous $NaSO_4$ column and the eluted solution was evaporated by a

stream of nitrogen. The dried methylated samples were detected by FT-IR spectroscopy to ensure that the peak of –O-H in the region 3500-3100 cm^{-1} had been eliminated. Then the per-methylated samples were hydrolyzed, reduced and acetylated as partially methylated alditol acetates (PMAA) which were further analyzed by GC-MS for linkage analysis. Aliquots of the PMAA were separated on a SP-2330 capillary column (30 m×0.25 mm I.D., 0.2 μm film thickness, Supelco, Bellefonte, PA, USA). The oven temperature was set initially at 160 ºC, increased at the rate of 2 ºC/min to 210 ºC, and then increased at 5 ºC/min to 240 ºC.

2.3.5 NMR spectrum

The polysaccharides (30 mg) were deuterium-exchanged three times and finally dissolved in 0.5 mL of D_2O (99.9% D). The ^{1}H and ^{13}C NMR spectra were measured on a Bruker Advance 400 MHz NMR spectrometer (Bruker, Rheinstetten, Germany) at 298 K. Acetone was used here as the internal standard (δ_H 2.225 ppm, δ_C 31.45 ppm), and Bruker TopSpin program was used to acquire and process the NMR data.

2.4. Immunomodulating effects determination

2.4.1. Cell cultures

The murine macrophage cell line RAW264.7 was obtained from American Type Culture

191 Collection (Manassas, VA) and was propagated in DMEM high glucose medium (Invitrogen
192 Life Technologies, Carlsbad, CA) supplemented with 10% heat-inactivated FBS (Gibco,
193 Carlsbad, CA, USA), 100 U/mL penicillin and 100 μg/mL streptomycin (Gibco, Carlsbad,
194 CA, USA).

195 *2.4.2. Cell viability assay*

196 The viability of cells was measured using MTT assay. Briefly, RAW264.7 cells (5×10^3
197 cells/well) were plated in 96-well microplates overnight and then treated with serial
198 concentrations of DOP, DOP-1 and DOP-2 for 24 h, respectively. Equal volume of medium
199 was used as vehicle control. After treatment, cells were stained with MTT at a final
200 concentration of 0.5 mg/mL in PBS (pH 7.4) for another 4 h in dark and then the medium was
201 discarded. The formazan crystals present in cells were dissolved by dimethyl sulfoxide. The
202 absorbance was read at 570 nm in a Benchmark Plus microplate reader (Bio-Rad, Richmond,
203 CA). The results were expressed as ratio of absorbance values of treatment to vehicle control
204 cells.

205 *2.4.3. ELISA for quantitative analysis of cytokines*

206 RAW264.7 cells (1×10^4 cells/well) were seeded in 96-well plates and incubated
207 overnight. Then, DOP and its two sub-fractions at 125, 250, and 500 μg/mL, respectively
208 (plus 10 mg/mL of polymyxin B for eliminating the functions of LPS) were added and the

209 cells were incubated for another 24 h. The cell supernatants were collected by centrifugation
210 at 1,000×g for 10 min. The amounts (pg/mL) of IL-6 and of TNF-α secretion in culture
211 supernatants were determined in duplicate by using an ELISA kit according to the
212 manufacturer's instructions. LPS (100 ng/mL) and LPS plus polymyxin B were used here as
213 controls.

214 *2.4.4. Phagocytic assay*

215 Dextran (M_w 12 kDa), which is characterized by low immunogenicity and high
216 resistance to cleavage, was fluorescein isothiocyanate-conjugated and prepared for the
217 phagocytic assay according to the published method (*22, 23*). RAW264.7 cells (4×10^5
218 cells/well) were seeded in 12-well plates overnight and then were exposed to cell culture
219 medium, serial concentrations of DOP, DOP-1 and DOP-2, and LPS for 24 h. Then the cells
220 were treated with FITC-dextran (0.1 mg/mL) and incubated for 1 h. After incubation, cells
221 were washed four times in cold PBS and were analyzed by flow cytometry (BD Biosciences,
222 USA).

223 *2.4.5. Lymphocyte proliferation assays*

224 Spleens were collected from 6-8 week-old BALB/c mice after killing them by cervical
225 dislocation. Single cell suspension of splenocytes was prepared according to the method

descried by Matsuzaki (*24*). Briefly, the spleens were cut into several pieces and pressed through 70 μm cell strainer (BD falcon, BD Biosciences, San Jose, CA) into culture medium using a syringe plunger. After centrifugation at 100×g for 10 min, cell pellets were washed twice with Hank's balanced salt solution (HBSS, Gibco, Carlsbad, CA, USA). Spleen cells were re-suspended in red cell lysis buffer in order to lyse red cells and incubated at room temperature for 5 min. The lymphocytes were collected and washed twice with RPMI-1640 without FBS. Proliferation of mouse spleen cells was measured using the lymphocyte transformation assay as previously described (*25, 26*). Briefly, the resulting pellet was re-suspended and diluted to 5×10^6 cells/mL with RPMI-1640 after the cell viability was assessed by trypan blue exclusion. The cell suspension was incubated in 96-well culture plates, 100 μL per well. The lymphocyte proliferation of *Dendrobium officinale* polysaccharides was tested by incubating the mouse splenocytes in the absence or presence of DOP, DOP-1, and DOP-2 at various concentrations for 48 h. It is known that LPS and Con A stimulate B cells and T cells, respectively. Thus, we used the optimal concentration of LPS (20 μg/mL) and Con A (1.25 μg/mL) as positive control compounds. After that, 20 μL of CellTiter 96® AQueous One Solution Cell Proliferation reagent was added into each well at 4 h before the end of incubation. The absorbance of cells in each well was measured by Benchmark Plus microplate reader (Bio-Rad, Richmond, CA) at a wave length of 490 nm, and the results of OD values were represented as mean ± SD.

To detect co-stimulatory activity of *Dendrobium officinale* polysaccharides and mitogenic stimulators (Con A and LPS), the mouse splenocytes were cultured with different concentrations of DOP, DOP-1, and DOP-2 (125, 250, and 500 μg/mL) and two different mitogens (Con A and LPS) at their predetermined optimal concentrations (Con A: 1.25 μg/mL; LPS: 20 μg/mL) for 48 h. Subsequent treatment and determinations were performed as described previously.

2.5. Data analysis

All data were expressed as mean ± SD. Statistical analysis was performed using one way ANOVA, and statistical significance was determined at $*p<0.05$, $**p<0.01$, $***p<0.001$, $**** p<0.0001$.

3. Results

3.1. Fractions and molecular characterization

As shown in Figure 1A, DOP was purified by ion-exchange chromatography on DEAE-650M. Two main fractions DOP-1 (eluted with ultrapure water) and DOP-2 (eluted with 0.01 M NaCl) were obtained, accounting for 66.4% and 23.6% of total polysaccharides by weight, respectively. They both exhibited high homogeneity in HPGPC examination (Figure 1B). The weight-average molecular weight (M_W) of the DOP and its two fractions

(DOP-1 and DOP-2) were close, which were found to be 7.3×10^5, 8.1×10^5, and 6.7×10^5 Da, respectively, which illustrated that DOP could be successfully separated into DOP-1 and DOP-2 by ion-exchange chromatography.

3.2. Chemical components and monosaccharide compositions

The chemical compositions of cDOP, DOP, DOP-1, and DOP-2 are summarized in Table 1. The average starch content of cDOP was 10.0%, while after de-starching with thermostable α-amylase, starch was not found in DOP, DOP-1, and DOP-2. A higher percentage of neutral sugar and lower percentages of protein and uronic acid were found in DOP, DOP-1, and DOP-2, as compared to cDOP.

DOP, DOP-1, and DOP-2 showed similar monosaccharide composition (Figure 1C). Only two monosaccharides were found, namely mannose (Man) and glucose (Glc). The mannose percentage, glucose percentage, and mannose/glucose ratios (M/G) are shown in Table 2. The mannose/glucose ratios for DOP, DOP-1, and DOP-2 were 5.8±0.1, 5.6±0.1, and 5.9±0.1, respectively.

3.3. Infrared spectroscopy

The FT-IR spectra of cDOP, DOP, DOP-1, and DOP-2 (Figure 1D) were similar. The broad and strong absorbance bands at 3436 cm^{-1} between the region 3500-3100 cm^{-1} can be

279 attributed to the vibration of hydroxyl groups of polysaccharides and water involved in
280 hydrogen bonding (*27*). The absorption at around 2891 cm^{-1} (3000-2800 cm^{-1}) was assigned
281 to the C-H stretching vibration of the methyl group (*28, 29*), and bonds approximately 1736
282 cm^{-1} were assigned to the valence vibration of C=O (*13*). Furthermore, peaks at around 1379
283 cm^{-1} and 1250 cm^{-1} were due to symmetric C-H bending vibration of the methyl group and
284 the C-O vibration of O-acetyl groups, respectively (*30*). The bonds at 878 cm^{-1} and 813 cm^{-1}
285 revealed the presence of β-$_D$-mannopyranose units and α-$_D$-galactopyranose units,
286 respectively (*31*). The assignment of the absorption peaks are given in Table 3, and are
287 consistent with the results of monosaccharide composition analysis (Table 2).

288 *3.4. Methylation and GC-MS analysis*

289 The major sugar residues and their positions at which they were substituted in the
290 polysaccharides were determined by methylation and GC-MS analysis. The individual
291 residues were qualitatively determined according to the retention times of their derivatives in
292 GC and by comparison of mass spectra with literature data (*20, 32*). The linkage patterns of
293 DOP and its two fractions are summarized in Table 4. They showed similar linkage modes,
294 mainly 1,4-linked mannosyl and 1,4-linked glucosyl units. It is suggested that DOP and its
295 two sub-fractions mainly comprise linear glucomannan. Meanwhile, a small number of
296 terminal groups (T-Man*p*) and branched residues 1,2,4-linked-Man*p*, 1,3,4-linked-Man*p*, and

297 1,4,6-linked-Man*p* were also found in DOP, DOP-1, and DOP-2, inferring that some terminal
298 mannosyl groups were attached to the *O*-2, *O*-4 and *O*-6 positions of 1,4-linked Man*p*.

299 *3.5. NMR spectroscopy*

300 The 1D ^{1}H and ^{13}C NMR spectra of DOP-1 and DOP-2 at 298 K are shown in Figure 2.
301 They look identical. Based on data in the literature (*13, 33, 34*), the signals at around δ_H 2.08
302 ppm and δ_C 21.54-21.81 ppm were assigned to the protons and methyl carbons in acetyl
303 groups. And the ^{13}C resonances at δ_C 173.79-173.83 ppm were assigned to carbonyl carbons
304 in *O*-acetyl groups. There were two peaks at around δ_C 103.75 and 101.40 ppm in the
305 anomeric region of ^{13}C NMR spectra of both DOP-1 and DOP-2 (Figure 2B); these belong to
306 β-1,4-linked Glc*p* and β-1,4-linked Man*p*, respectively. The results above indicate that both
307 DOP-1 and DOP-2 have a backbone of 1,4-linked β-$_D$-mannopyranosyl and
308 β-$_D$-glucopyranosyl residues, which is consistent with the results of methylation analysis.
309 In summary, we conclude that the structures of DOP-1 and DOP-2 are similar to each
310 other. The backbones of the two polysaccharides consist of units of
311 β-$_D$-Man*p*-(1→4)-β-$_D$-Glc*p*-(1→.

312 *3.6. Effects of DOP and its two sub-fractions on proliferation of RAW264.7 cells*

313 The cell proliferation effects of DOP and its two fractions on RAW264.7 cells are shown

314 in Figure 3A. When administered at varied concentrations of 3.75, 7.5, 15, 30, 62, 125, 250,
315 500, and 1000 μg/mL together with polymyxin B (10 μg/mL), DOP and its two fractions
316 induced cell proliferation but polymyxin B did not inhibit it. However, the effect of LPS was
317 excluded by polymyxin B. DOP had significant proliferation effects at different
318 concentrations from 3.75 to 1000 μg/mL. The proliferation rate increased along with the
319 concentration from 3.75 μg/mL to 125 μg/mL (p<0.0001), but declined to the control value at
320 the high concentration of 1000 μg/mL. Similar results were also observed for DOP-1 and
321 DOP-2. In summary, none of DOP, DOP-1, and DOP-2 showed cytotoxicity on RAW264.7
322 cells. Therefore, the three concentrations of 125, 250, and 500 μg/mL were chosen for further
323 study.

324 *3.7. Effects of DOP and its two sub-fractions on cytokine production of RAW 264.7 cells*

325 As shown in Figure 3B, DOP, DOP-1, and DOP-2 exhibited similar effects on the
326 TNF-α production of RAW 264.7 cells with the positive control LPS. The effect of LPS was
327 suppressed by polymyxin B, but polymyxin B did not inhibit TNF-α production of DOP and
328 its two fractions. The effect on TNF-α production of DOP, DOP-1, and DOP-2 was
329 dose-dependent at the concentrations of 125, 250, and 500 μg/mL. All of DOP, DOP-1, and
330 DOP-2 had little effect on NO and IL-6 production (data not shown).

331 *3.8. Phagocytic activities of DOP and its two sub-fractions*

As shown in Figure 3C, the positive control LPS significantly increased the phagocytosis rate of RAW264.7 cells at the concentrations of 2 μg/mL, while polymyxin B inhibited this effect. DOP, DOP-1, and DOP-2 all exhibited similar inducing effects in a dose-dependent manner at the concentrations of 125, 250, and 500 μg/mL, but polymyxin B did not suppress their effects. DOP significantly increased phagocytosis rates from 18.3±0.42% (125 μg/mL, $p<0.001$) to 26.6±1.70% (500 μg/mL, $p<0.0001$), and comparable activities were also observed in groups of DOP-1 and DOP-2.

3.9. Proliferation of mouse spleen lymphocytes after stimulation with DOP and its two sub-fractions

As shown in Figure 4A, Con A and LPS significantly triggered T lymphocyte and B lymphocyte proliferation, respectively, and these results were consistent with previous studies (*35, 36*). *DOP and its two sub-fractions* also stimulated lymphocyte proliferation *in vitro*. The OD490 values of DOP, DOP-1, and DOP-2 groups were significantly higher than that of the control group at concentrations of 125, 250, and 500 μg/mL.

3.10. Changes of T and B lymphocyte proliferation in synergistical stimulation by DOP and its two sub-fractions with mitogen

As shown in Figure 4B, the OD490 values of DOP and its two sub-fractions groups were

significantly higher than that of the cell control group, and rose in a dose-dependent manner at the concentrations of 125, 250, and 500 μg/mL. Compared to the value of positive control LPS group, DOP, DOP-1, and DOP-2 co-cultured with LPS groups also significantly increased OD490 values at the concentrations of 125 250, and 500 μg/mL. DOP-2 displayed significant mitogenic activity on mouse lymphocytes, yet it did not have significant proliferation effect at the concentration of 125 μg/mL as compared to the LPS group. When co-cultured with *D. officinale* polysaccharides, the lympho-proliferative response induced by optimal concentration of Con A (1.25 μg/mL) was significantly enhanced (Figure 4C) compared with the Con A-stimulating group and control group in a dose-dependent manner.

4. Discussion

Teipi Shihu has a complicated chemical profile. In addition to bibenzyls, phenanthrenes, sesquiterpenoids, and other small compounds, polysaccharides are the dominant component, with content up to 50% of the total dry weight (*37*). In our previous study (*12*), we demonstrated the molecular size distribution pattern of the water extract of *Teipi Shihu*, and found DOP to be the unique polysaccharide marker with its content being close to 30% of the total dry weight. There are also some other polysaccharides, in addition to DOP.

Five polysaccharide fractions have been obtained from *D. officinale* through a sequential ethanol precipitation method (*38*). Another study using anion-exchange chromatography on

DEAE-cellulose (NH_2) separated six fractions from a crude *D. officinale* polysaccharide (*39, 40*). Despite the differences in molecular weights, mannose-to-glucose ratios, and number of acetyl groups, all these polysaccharides are types of acetyl-glucomannan. In our study, DOP and its two sub-fractions also showed the identical general features: acetyl-glucomannan having a high degree of polymerization and a limited degree of branching.

Up to now, only two studies have reported the structural details of de-starched and HPGPC-homogenous 2-*O*-acetyl-glucomannan isolated from *D. officinale* (*13, 39*). Comparison with these literature data reveals some similarities and differences between these reported polysaccharides and the *Dendrobium officinale* polysaccharides in our study. Consistent with data in the literature (*13, 39*), our data also indicates that the backbone of DOP-1 and DOP-2 has (1→4)-linked β-$_D$-mannopyranosyl residues and β-$_D$-glucopyranosyl residues. Both the literature and our studies show identical 1D NMR spectra. But, in our results, the *Mw* of DOP-1 and DOP-2 (8.1×10^5 and 6.7×10^5 Da, respectively) was a bit larger than the data in the literature (*13, 39, 40*). The reported polysaccharides also contained traces of arabinose (*39*) or galactose and arabinose (*13, 40*). However, we found no monosaccharides other than mannose and glucose in DOP-1 and DOP-2.

The chemical structures of these polysaccharides have not been directly confirmed by high-quality 2D NMR spectra. In order to obtain a high-quality NMR spectrum, the polysaccharide sample needs to be dissolved in D_2O or DMSO to form a homogenous

386 solution at the concentrations of approximate 3–4% (w/v). But *Dendrobium* polysaccharides
387 including DOP-1 and DOP-2 in the present study always have high viscosity and relatively
388 low solubility in D_2O. Therefore it is hard to get their high-quality 2D NMR spectra. A
389 previous study also encountered this problem (*13*). In that case, the authors had to degrade
390 their polymer sample using endo-β-mannanase, and tried to characterize the chemical
391 structure by analyzing the major enzyme-hydrolysis products for which 1D/2D NMR spectra
392 are satisfactory.

393 Natural polysaccharides isolated from *D. officinale* have been shown to possess various
394 bioactivities, especially the effect to modulate immune function (*3, 40-43*). Our results
395 regarding the immunomodulatory activity of DOP and its two fractions indicate that *D.*
396 *officinale* polysaccharides exert significant immunomodulatory effects on innate immune
397 responses mediated by spleen lymphocytes and macrophages. They significantly stimulated
398 the proliferation of splenocytes which is related to immunity improvement of T-lymphocytes
399 and/or B-lymphocytes (Marciani et al., 2000). Therefore, DOP-1 and DOP-2 can be
400 considered pharmaceutically active components of DOP extracted from *D. officinale.*

401 Known to be one of the target cells of polysaccharides, macrophages represent the first
402 line of host defense (*44*) and are the most important antigen-presenting cells. Macrophages
403 possess many immune functions, such as phagocytosis, antigen processing, and cytokine
404 production (*45*). Macrophages are in a state of dormancy and their functions can be activated

405 by immunoenhancers (*46*). One of the most useful indicators of macrophage activation would
406 be an enhancement of phagocytic activity, which represents a vital step in the immunological
407 defense system. Consistent with previous studies, our results demonstrate that all
408 polysaccharides in *D. officinale* increase macrophages' phagocytic activity significantly (*42*).
409 Administration of DOP may result in the initiation of an immune reaction against foreign
410 pathogens and tumors. Apart from the phagocytosis, activated macrophages accompanied by
411 TNF-α production also play an important role in anti-tumor activity (*47, 48*). In this study, *D.*
412 *officinale* polysaccharides induced production of TNF-α in macrophages in a dose-dependent
413 manner. This result is in agreement with the previous study (*40, 42*).

414 Some reports in the literature have showed that polysaccharides in *D. officinale* induce
415 NO production (*40, 42*) and IL-6 production (*42*); however, increase in NO and IL-6
416 production was not detected in our studies. The immunomodulating activities of
417 polysaccharides are associated with their chemical composition, molecular weight,
418 conformation, glycosidic linkage, degree of branching and so on (*49, 50*). From these aspects,
419 our polysaccharides should contain some differences from those of the previous studies. In
420 this study, DOP and its two sub-fractions were found to contain the same monosaccharide
421 composition, identical linkage pattern, and similar degree of branching. This might explain
422 why they showed similar effects on RAW264.7 cells and spleen lymphocytes.

423 In conclusion, the unique polysaccharide marker DOP of *D. officinale* was separated

424 into two purified polysaccharides DOP-1 and DOP-2. DOP and its two sub-fractions showed
425 identical chemical structures with slightly different molecular weights. Furthermore, they all
426 have significant immunomodulatory activity *in vitro*, including activation of macrophages
427 and lymphocytes. DOP-1 and DOP-2 are thus proven to be major, active polysaccharide QC
428 markers of *D. officinale*.

429 **Acknowledgements**

430 This study was supported by HKSAR Innovation and Technology Fund (ITF), Tier 3,
431 ITS/311/09, and Hong Kong Baptist University (RC-start up grant, MPCF-001-2014/2015,
432 and FRG2/14-15/028).

433 **Conflict of Interest**

434 The authors declare no conflict of interest.
435

References

1. Zhang, G. N.; Bi, Z. M.; Wang, Z. T.; Xu, L. S.; Xu, G. J. Advances in studies on chemical constitutents from plants of *Dendrobium* Sw.. *Chin. Tradit. Herb. Drugs* **2003,** *6*, 041.

2. Deng, Y.; Xu, K.; Tan, G. Advances in studies on chemical constitutents and pharmacological activities of plants of *Dendrobium* Sw. *Chin. Tradit. Herb. Drugs* **2002,** *25*, 677-680.

3. Ng, T. B.; Liu, J.; Wong, J. H.; Ye, X.; Wing Sze, S. C.; Tong, Y.; Zhang, K. Y. Review of research on *Dendrobium*, a prized folk medicine. *Appl. Microbiol. Biotechnol.* **2012,** *93*, 1795-803.

4. Sun H. F. A Study on the Principles of the Prescription of Antipyretic and Heat-relieving Medicated Diets and Food Therapy and Their Cooking Characteristics. *Cuisine J. of Yangzhou University* **2005,** *2*, 009.

5. Wang, W.; Zou, H.; Chen, Y.; Lin, J. Utilization and prospection of *Dendrobium officinale*. *Chin. Horticulture Abstracts* **2011,** *1*, 189-192.

6. Zhang, Y. B.; But, P. P. H.; Wang, Z. T.; Shaw, P. C. Current approaches for the authentication of medicinal *Dendrobium* species and its products. *Plant Genetic Resources: Characterization and Utilization* **2005,** *3*, 144-148.

7. Kuang, H.; Xia, Y.; Liang, J.; Yang, B.; Wang, Q.; Sun, Y. Fast classification and compositional analysis of polysaccharides from TCMs by ultra-performance liquid

455 chromatography coupled with multivariate analysis. *Carbohydr. Polym.* **2011,** *84*, 1258-1266.

456 8. Zha, X. Q.; Luo, J. P.; Wei, P. Identification and classification of *Dendrobium candidum*

457 species by fingerprint technology with capillary electrophoresis. *South African J. Botany* **2009,**

458 *75*, 276-282.

459 9. Wang, L.; Wang, C.; Pan, Z.; Sun, Y.; Zhu, X. Application of pyrolysis-gas chromatography

460 and hierarchical cluster analysis to the discrimination of the Chinese traditional medicine

461 *Dendrobium candidum* Wall. ex Lindl. *J. Anal. Applied Pyrolysis* **2011,** *90*, 13-17.

462 10. Xu, J.; Guan, J.; Chen, X.; Zhao, J.; Li, S. Comparison of polysaccharides from different

463 *Dendrobium* using saccharide mapping. *J. Pharmaceutical Biomedi. Anal.* **2011,** *55*, 977-983.

464 11. Xu, J.; Zhao, W. M.; Qian, Z. M.; Guan, J.; Li, S. P. Fast determination of five components

465 of coumarin, alkaloids and bibenzyls in *Dendrobium* spp. using pressurized liquid extraction

466 and ultra-performance liquid chromatography. *J. Separa. Sci.* **2010,** *33*, 1580-1586.

467 12. Xu, J.; Li, S. L.; Yue, R. Q.; Ko, C. H.; Hu, J. M.; Liu, J.; Ho, H. M.; Yi, T.; Zhao, Z. Z.; Zhou, J.;

468 Leung, P. C.; Chen, H. B.; Han, Q. B. A novel and rapid HPGPC-based strategy for quality

469 control of saccharide-dominant herbal materials: *Dendrobium officinale*, a case study. *Anal.*

470 *Bioanal. Chem.* **2014,** *406*, 6409-17.

471 13. Xing, X.; Cui, S. W.; Nie, S.; Phillips, G. O.; Goff, H. D.; Wang, Q. Study on *Dendrobium*

472 *officinale* O-acetyl-glucomannan (Dendronan®): Part I. Extraction, purification, and partial

473 structural characterization. *Bioactive Carbohydr. Dietary Fibre* **2014,** *4*, 74-83.

14. Dubois, M.; Gilles, K. A.; Hamilton, J. K.; Rebers, P.; Smith, F. Colorimetric method for determination of sugars and related substances. *Anal. Chem.* **1956,** *28*, 350-356.

15. Tang, Y.; Yang, S.; Yan, Q.; Zhou, P.; Cui, J.; Jiang, Z. Purification and characterization of a novel β-1, 3–1, 4-glucanase (lichenase) from thermophilic Rhizomucor miehei with high specific activity and its gene sequence. *J. Agric. Food Chem.* **2012,** *60*, 2354-2361.

16. McCready, R. M.; McComb, E. A. Enzymes, Course of Action of Polygalacturonase on Polygalacturonic Acids. *J. Agri. Food Chem.* **1953,** *1*, 1165-1168.

17. Hou, W. C.; Lee, M. H.; Chen, H. J.; Liang, W. L.; Han, C. H.; Liu, Y. W.; Lin, Y. H. Antioxidant activities of dioscorin, the storage protein of yam (Dioscorea batatas Decne) tuber. *J. Agri. Food Chem.* **2001,** *49*, 4956-4960.

18. Yang, N.; Ren, G. Determination of D-chiro-Inositol in tartary buckwheat using high-performance liquid chromatography with an evaporative light-scattering detector. *J. Agri. Food Chem.* **2008,** *56*, 757-760.

19. Carre, B.; Brillouet, J. M.; Thibault, J. F. Characterization of polysaccharides from white lupine (Lupinus albus L.) cotyledons. *J. Agri. Food Chem.* **1985,** *33*, 285-292.

20. Nie, S. P.; Cui, S. W.; Phillips, A. O.; Xie, M. Y.; Phillips, G. O.; Al-Assaf, S.; Zhang, X. L. Elucidation of the structure of a bioactive hydrophilic polysaccharide from *Cordyceps sinensis* by methylation analysis and NMR spectroscopy. *Carbohydr. Polym.* **2011,** *84*, 894-899.

493 21. Zhang, H.; Nie, S. P.; Yin, J. Y.; Wang, Y. X.; Xie, M. Y. Structural characterization of a
494 heterogalactan purified from fruiting bodies of *Ganoderma atrum*. *Food Hydrocolloids* **2014,**
495 *36*, 339-347.
496 22. Li, E. W.; Mine, Y. Immunoenhancing effects of bovine glycomacropeptide and its
497 derivatives on the proliferative response and phagocytic activities of human macrophagelike
498 cells, U937. *J. Agri. Food Chem.* **2004,** *52*, 2704-2708.
499 23. Chuang, W. C.; Ho, Y. C.; Liao, J. W.; Lu, F. J. *Dunaliella salina* exhibits an antileukemic
500 immunity in a mouse model of WEHI-3 leukemia cells. *J. Agri. Food Chem.* **2014,** *62*,
501 11479-11487.
502 24. Matsuzaki, C.; Hayakawa, A.; Matsumoto, K.; Katoh, T.; Yamamoto, K.; Hisa, K.
503 Exopolysaccharides produced by leuconostoc mesenteroides strain NTM048 as an
504 immunostimulant to enhance the mucosal barrier and influence the systemic immune
505 eesponse. *J. Agri. Food Chem.* **2015,** *63*, 7009-7015.
506 25. Schauss, A. G.; Wu, X.; Prior, R. L.; Ou, B.; Huang, D.; Owens, J.; Agarwal, A.; Jensen, G.
507 S.; Hart, A. N.; Shanbrom, E. Antioxidant capacity and other bioactivities of the freeze-dried
508 Amazonian palm berry, Euterpe oleraceae mart.(acai). *J. Agri. Food Chem.* **2006,** *54*,
509 8604-8610.
510 26. Tong, H.; Song, X.; Sun, X.; Sun, G.; Du, F. Immunomodulatory and antitumor activities
511 of grape seed proanthocyanidins. *J. Agri. Food Chem.* **2011,** *59*, 11543-11547.

512 27. Sun, Y. D.; Wang, Z. H.; Ye, Q. S. Composition analysis and anti-proliferation activity of
513 polysaccharides from *Dendrobium chrysotoxum*. *Int. J. Biol. Macromol.* **2013,** *62*, 291-5.
514 28. Kang, J.; Cui, S. W.; Chen, J.; Phillips, G. O.; Wu, Y.; Wang, Q. New studies on gum ghatti
515 (Anogeissus latifolia) part I. Fractionation, chemical and physical characterization of the gum.
516 *Food hydrocolloids* **2011,** *25*, 1984-1990.
517 29. Buriti, F. C.; dos Santos, K. M.; Sombra, V. G.; Maciel, J. S.; Sá, D. M. T.; Salles, H. O.;
518 Oliveira, G.; de Paula, R. C.; Feitosa, J. P.; Moreira, A. C. M. Characterisation of partially
519 hydrolysed galactomannan from Caesalpinia pulcherrima seeds as a potential dietary fibre.
520 *Food Hydrocolloids* **2014,** *35*, 512-521.
521 30. Cerqueira, M. A.; Souza, B. W.; Simões, J.; Teixeira, J. A.; Domingues, M. R. M.; Coimbra,
522 M. A.; Vicente, A. A. Structural and thermal characterization of galactomannans from
523 non-conventional sources. *Carbohydr. Polym.* **2011,** *83*, 179-185.
524 31. Albuquerque, P. B.; Barros, W.; Santos, G. R.; Correia, M. T.; Mourão, P. A.; Teixeira, J. A.;
525 Carneiro-da-Cunha, M. G. Characterization and rheological study of the galactomannan
526 extracted from seeds of *Cassia grandis*. *Carbohydr. Polym.* **2014,** *104*, 127-134.
527 32. Carpita, N. C.; Shea, E. M., Linkage structure of carbohydrates by gas
528 chromatography-mass spectrometry (GC-MS) of partially methylated alditol acetates. *Anal.*
529 *Carbohydr. by GLC and MS* **1989**, 157-216.
530 33. Hannuksela, T.; du Penhoat, C. H. NMR structural determination of dissolved

O-acetylated galactoglucomannan isolated from spruce thermomechanical pulp. *Carbohydr. Res.* **2004,** *339*, 301-312.

34. Lundqvist, J.; Teleman, A.; Junel, L.; Zacchi, G.; Dahlman, O.; Tjerneld, F.; Stålbrand, H. Isolation and characterization of galactoglucomannan from spruce (Picea abies). *Carbohydr. Polym.* **2002,** *48*, 29-39.

35. Palacios, R. Concanavalin A triggers T lymphocytes by directly interacting with their receptors for activation. *J. Immunol.* **1982,** *128*, 337-42.

36. Mamchak, A. A.; Hodgkin, P. D. Regulation of lipopolysaccharide-induced B-cell activation: evidence that surface immunoglobulin mediates two independently regulated signals. *Immunol. Cell Bio.* **2000,** *78*, 142-8.

37. Xu, J.; Han, Q. B.; Li, S. L.; Chen, X. J.; Wang, X. N.; Zhao, Z. Z.; Chen, H. B. Chemistry, bioactivity and quality control of *Dendrobium*, a commonly used tonic herb in traditional Chinese medicine. *Phytochemistry Reviews* **2013,** *12*, 341-367.

38. Xing, X.; Cui, S. W.; Nie, S.; Phillips, G. O.; Douglas Goff, H.; Wang, Q. A review of isolation process, structural characteristics, and bioactivities of water-soluble polysaccharides from *Dendrobium* plants. *Bioactive Carbohydrates and Dietary Fibre* **2013,** *1*, 131-147.

39. Hua, Y. F.; Zhang, M.; Fu, C. X.; Chen, Z. H.; Chan, G. Y. Structural characterization of a 2-O-acetylglucomannan from *Dendrobium officinale* stem. *Carbohydr. Res.* **2004,** *339*,

550 2219-24.

551 40. Xia, L.; Liu, X.; Guo, H.; Zhang, H.; Zhu, J.; Ren, F. Partial characterization and
552 immunomodulatory activity of polysaccharides from the stem of *Dendrobium officinale*
553 (Tiepishihu) *in vitro*. *J. Func. Foods* **2012,** *4*, 294-301.

554 41. Huang, X.; Nie, S.; Cai, H.; Zhang, G.; Cui, S. W.; Xie, M.; Phillips, G. O. Study on
555 *Dendrobium officinale* O-acetyl-glucomannan (Dendronan): Part IV. Immunomodulatory
556 activity *in vivo*. *J. Func. Foods* **2015,** *15*, 525-532.

557 42. Cai, H. I.; Huang, X. J.; Nie, S. P.; Xie, M. Y.; Phillips, G. O.; Cui, S. W. Study on
558 *Dendrobium officinale* O-acetyl-glucomannan (Dendronan®): Part III–Immunomodulatory
559 activity *in vitro*. *Bioactive Carbohydrates and Dietary Fibre* **2015,** *5*, 99-105.

560 43. Liu, X. F.; Zhu, J.; Ge, S. Y.; Xia, L. J.; Yang, H. Y.; Qian, Y. T.; Ren, F. Z. Orally administered
561 *Dendrobium officinale* and its polysaccharides enhance immune functions in BALB/c mice.
562 *Nat. Prod. Commun.* **2011,** *6*, 867-70.

563 44. Schepetkin, I. A.; Quinn, M. T. Botanical polysaccharides: macrophage
564 immunomodulation and therapeutic potential. *Int. Immunopharmacol.* **2006,** *6*, 317-33.

565 45. Elhelu, M. A. The role of macrophages in immunology. *J. Natl. Med. Assoc.* **1983,** *75*,
566 314-7.

567 46. Mosser, D. M. The many faces of macrophage activation. *J. Leukoc. Biol.* **2003,** *73*,
568 209-12.

569 47. Haranaka, K.; Satomi, N.; Sakurai, A. Antitumor activity of murine tumor necrosis factor
570 (TNF) against transplanted murine tumors and heterotransplanted human tumors in nude
571 mice. *Int. J. Cancer* **1984,** *34*, 263-267.
572 48. van Horssen, R.; ten Hagen, T. L.; Eggermont, A. M. TNF-α in cancer treatment:
573 molecular insights, antitumor effects, and clinical utility. *The oncologist* **2006,** *11*, 397-408.
574 49. Methacanon, P.; Madla, S.; Kirtikara, K.; Prasitsil, M. Structural elucidation of bioactive
575 fungi-derived polymers. *Carbohydr. Polym.* **2005,** *60*, 199-203.
576 50. Yadomae, T.; Ohno, N., Structure-activity relationship of immunomodulating (1→
577 3)-beta-d-glucans. *Recent Res. Dev. Chem. Pharm. Sci.* **1996,** *1*, 23-33.
578
579
580 **Figure Captions**
581
582 **Figure 1. (A)** Chromatogram of the polysaccharides from *Dendrobium officinale* on
583 ion-exchange column (DEAE-650M). **(B)** HPGPC chromatogram of cDOP (crude DOP),
584 DOP (non-starch DOP), DOP-1 (non-starch DOP-1), and DOP-2 (non-starch DOP-2) (c=2.0
585 mg/mL). **(C)** HPLC-ELSD chromatogram of standard monosaccharide mixture and
586 hydrolysis products of mixed standards, DOP, DOP-1, and DOP-2. Black line: Standard
587 mixture of mannose (Man, c=1.6 mg/mL) and glucose (Glc, c=1.6 mg/mL). **(D)** FT-IR
588 spectra of cDOP, DOP, DOP-1, and DOP-2.

589 **Figure 2**. ^{1}H (**A**) and ^{13}C (**B**) NMR spectra of DOP-1 and DOP-2, obtained at 298 K.

590 **Figure 3**. Effects of DOP, DOP-1, and DOP-2 on the cell viability (**A**), TNF-α production (**B**),
591 and phagocytosis activity (**C**) of RAW264.7 cells.
592 Mouse macrophages RAW264.7 cells were treated with different concentrations of DOP,
593 DOP-1, and DOP-2, positive control LPS, LPS plus polymyxin B (10 μg/mL) or vehicle for
594 24 h. MTT method, ELISA assay, and FACScan flow cytometry were used for analyzing cell
595 viability, TNF-α production, and phagocytosis rate, respectively. The data are presented as the
596 mean±SD. *p<0.05, **p<0.01, ***p<0.0001, ****p<0.0001 compared with the control
597 group.

598 **Figure 4**. Proliferation of lymphocytes after stimulation by DOP, DOP-1, and DOP-2 at
599 different concentrations and/or mitogen (LPS or Con A). (**A**) Lymphocytes (5×105 cells/well)
600 in 96-well-plate were incubated with DOP, DOP-1, and DOP-2 at different concentrations for
601 48 h. Two positive controls were used: LPS (20 μg/mL), a lipopolysaccharide which is a
602 mitogen of B cells, and Con A (1.25 μg/mL), a phytohemagglutinin which is a mitogen of T
603 cells. (**B** and **C**) Lymphocytes (5×105 cells/well) were treated by LPS/Con A with or without
604 DOP, DOP-1, and DOP-2 at the indicated concentrations for 48 h. The cell viability was
605 measured with tetrazolium compound (MTS) method. The different DOP and mitogens were
606 dissolved and applied in medium. Control cells were treated with medium. The data are
607 presented as the mean±SD. *p<0.05, **p<0.01, ***p<0.001, **** p<0.0001 compared with

608 the control group.

609 **Table 1** Chemical compositions of CDOP, DOP, DOP-1, and DOP-2.

610 **Table 2** Monosaccharide analysis of DOP, DOP-1, and DOP-2.

611 **Table 3** FT-IR spectra of DOP, DOP-1, and DOP-2: wave numbers and intensities of

612 functional groups.

613 **Table 4** Glycosyl-linkage analysis of DOP, DOP-1, and DOP-2.

614

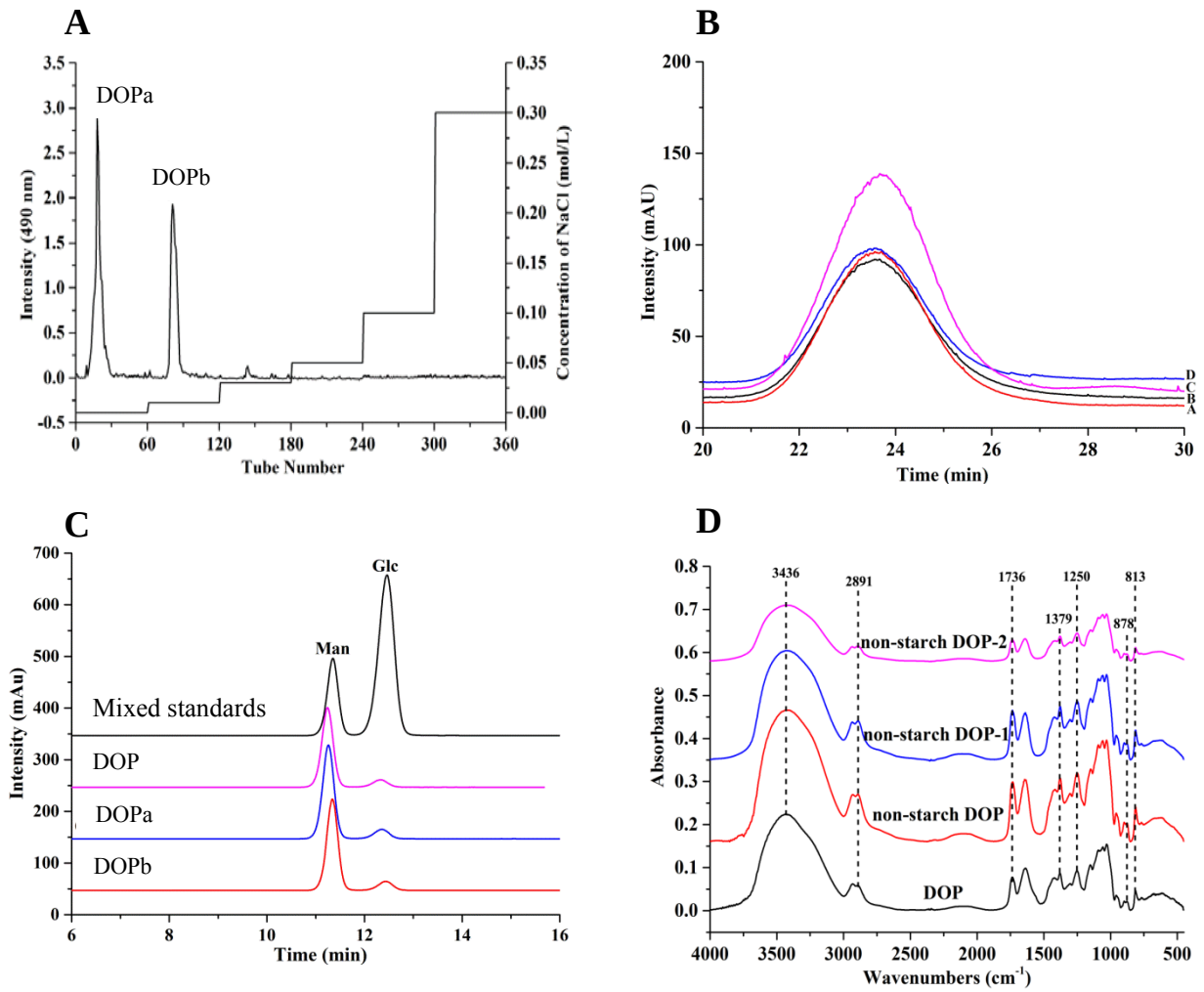

Figure 1. (**A**) Chromatogram of the polysaccharides from *Dendrobium officinale* on ion-exchange column (DEAE-650M). (**B**) HPGPC chromatogram of DOP, DOPa, and DOPb (C=2.0 mg/ml). (**C**) HPLC-ELSD chromatogram of standard monosaccharide mixture and hydrolysis products of DOP, DOPa, and DOPb. : Standard mixture of mannose (Man, c=1.6 mg/ml) and glucose (Glc, c=1.6 mg/ml); : DOPb; : DOPa; : DOP (**D**) FT-IR spectra of CDOP, DOP, DOPa, and DOPb.

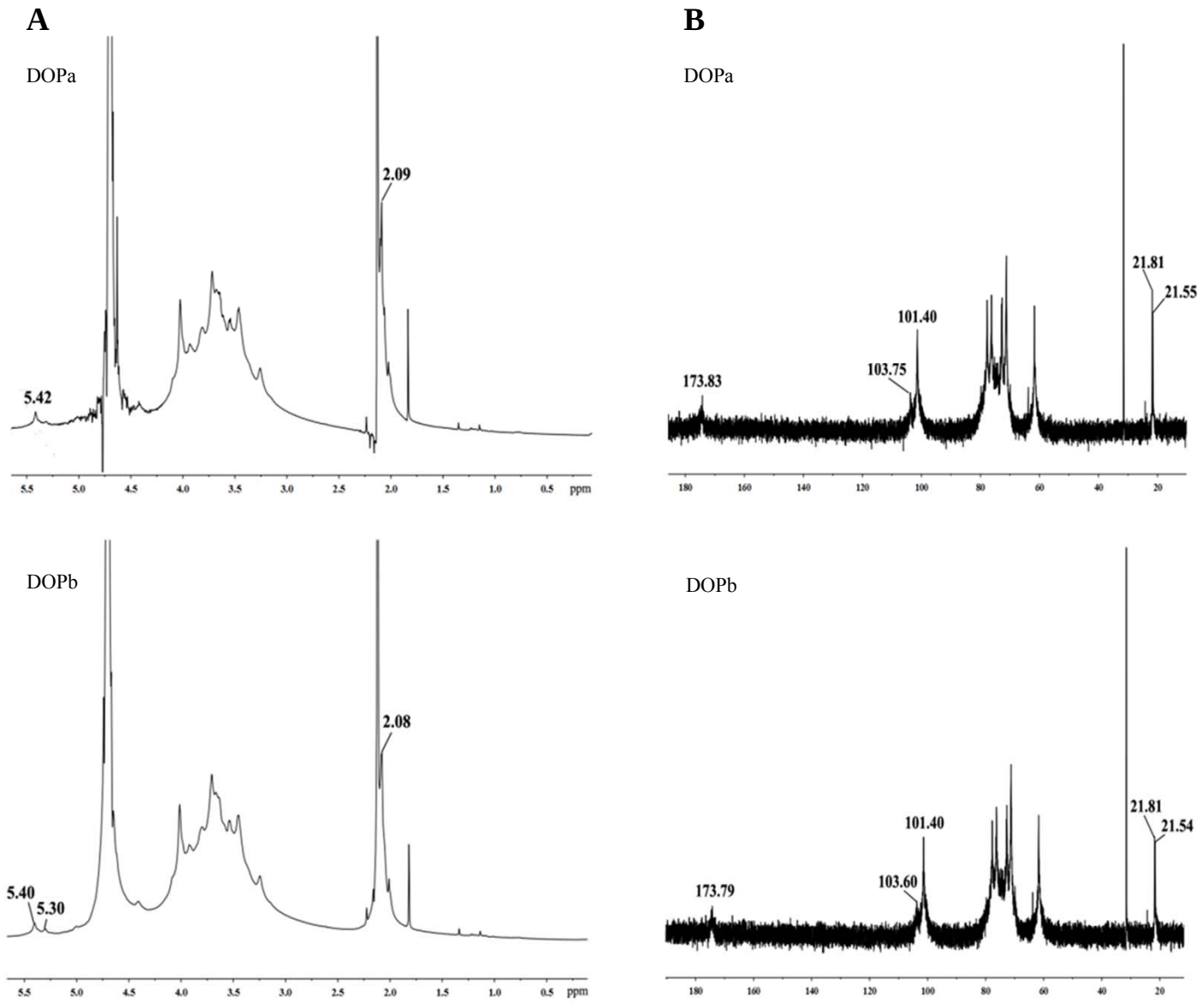

Figure 2. ^{1}H (**A**) and ^{13}C (**B**) NMR spectra of DOPa and DOPb, obtained at 298 K.

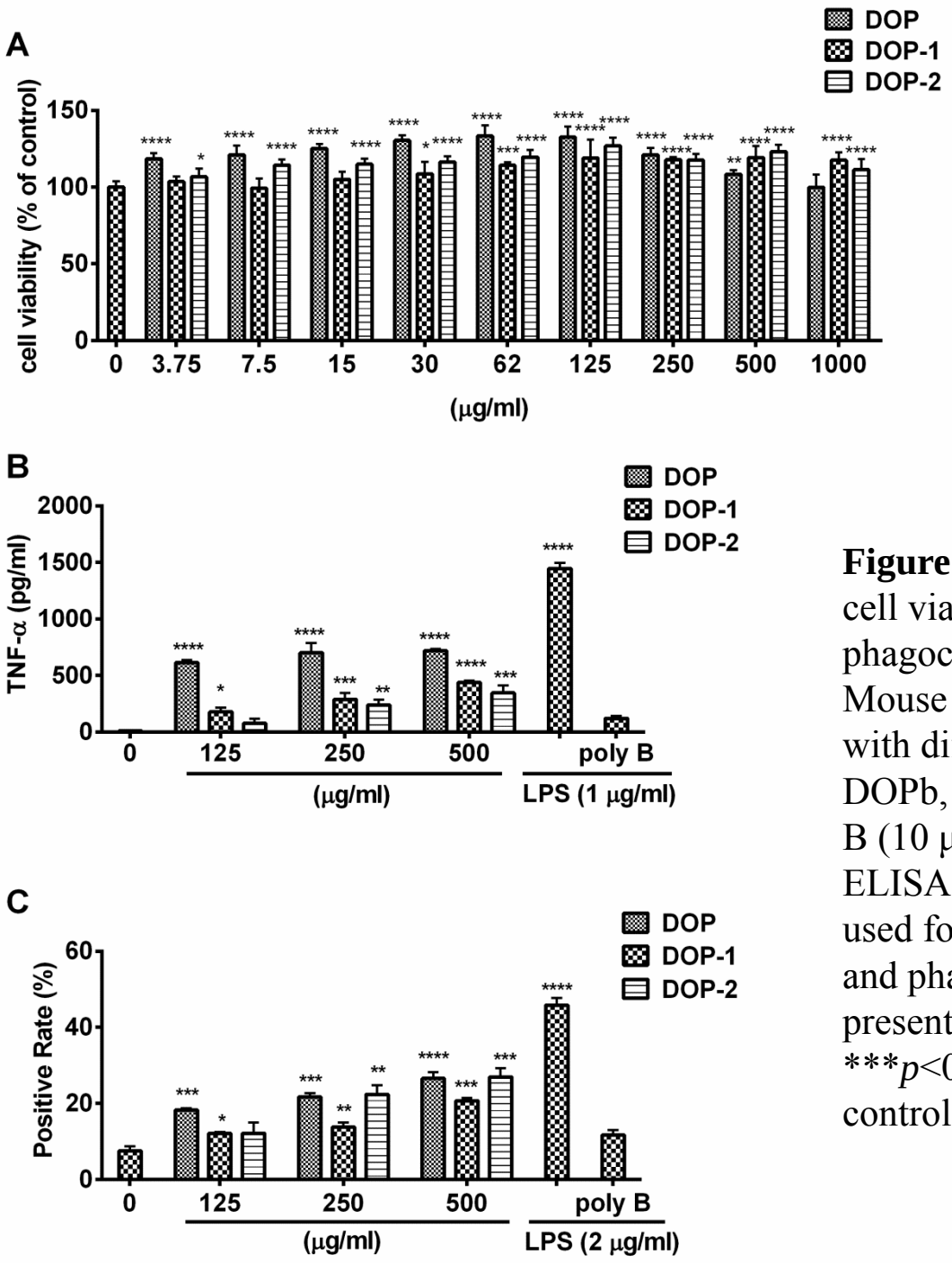

Figure 3. Effects of DOP, DOPa, and DOPb on the cell viability (**A**), TNF-α production (**B**), and phagocytosis activity (**C**) of RAW264.7 cells. Mouse macrophages RAW264.7 cells were treated with different concentrations of DOP, DOPa, and DOPb, positive control LPS, LPS plus polymyxin B (10 μg/ml) or vehicle for 24 h. MTT method, ELISA assay, and FACScan flow cytometry were used for analyzing cell viability, TNF-α production, and phagocytosis rate, respectively. The data are presented as the mean±SD. *p<0.05, **p<0.01, ***p<0.0001, ****p<0.0001 compared with the control group.

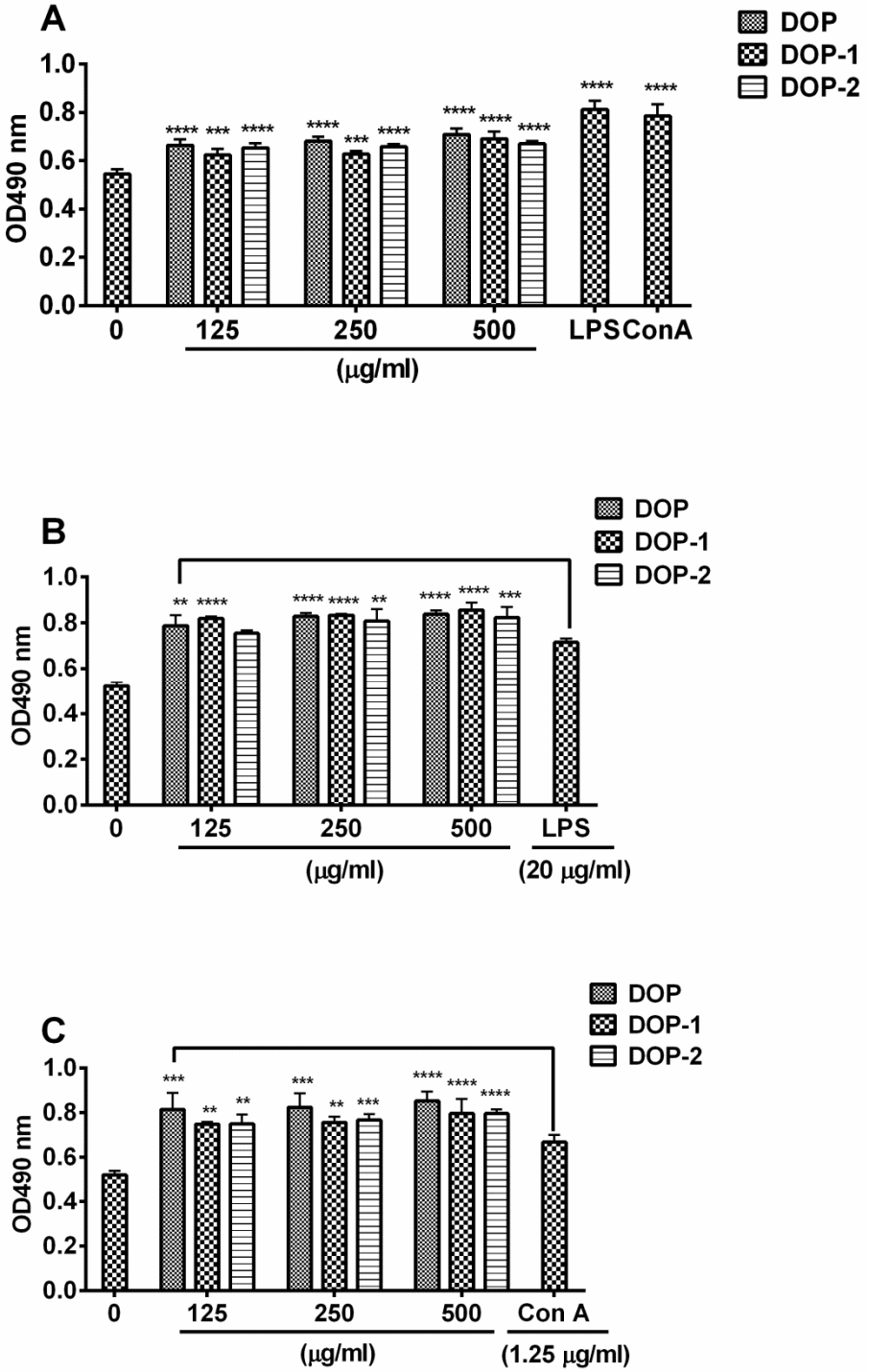

Figure 4. Proliferation of lymphocytes after stimulation by DOP, DOPa, and DOPb at different concentrations and/or mitogen (LPS or Con A). (**A**) Lymphocytes (5×10^5 cells/well) in 96-well-plate were incubated with DOP, DOPa, and DOPb at different concentrations for 48 h. Two positive controls were used: LPS (20 mg/ml), a lipopolysaccharide which is a mitogen of B cells, and Con A (1.25 mg/ml), a phytohemagglutinin which is a mitogen of T cells. (**B** and **C**) Lymphocytes (5×10^5 cells/well) were treated by LPS/Con A with or without DOP, DOPa, and DOPb at the indicated concentrations for 48 h. The cell viability were measured with tetrazolium compound (MTS) method. The different DOP and mitogens were dissolved and applied in medium. Control cells were treated with medium. The data are presented as the mean±SD. *$p<0.05$, **$p<0.01$, ***$p<0.001$, **** $p<0.0001$ compared with the control group.

Table 1 Chemical compositions of CDOP, DOP, DOPa, and DOPb

	CDOP	DOP	DOPa	DOPb
Total starch (%) [a]	10.0 ± 0.60[b]	ND[c]	ND	ND
Netural Sugar (%)	76.5 ± 6.9	92.5 ± 4.1	93.4 ± 8.0	92.1 ± 2.0
Protein (%)	4.79 ± 0.52	1.49 ± 0.50	1.39 ± 0.33	1.66 ± 0.12
Total uronic acid (%)	2.31 ± 0.01	2.15 ± 0.24	2.04 ± 0.10	1.93 ± 0.20

[a] %: molar percentage

[b] Data was shown as mean±SD (n=3)

[c] ND: not detectable or lower than limits of quantification

Table 2 Monosaccharide analysis of DOP, DOPa, and DOPb

Sample	Mannose (%, w/w)[a]	Glucose (%, w/w)	Mannose/Glucose
DOP	85.2 ± 0.54	14.8 ± 0.24	5.78 ± 0.11
DOPa	84.8 ± 0.16	15.2 ± 0.06	5.59 ± 0.03
DOPb	85.5 ± 0.62	14.5 ± 0.02	5.92 ± 0.01

[a]: Data were shown as mean±SD, (n=3)

Table 3 FT-IR spectra of DOP, DOPa, and DOPb: wave numbers and intensities of functional groups.

Wavenumbers (cm^{-1})	Functional groups
3436	Vibration of O-H
2891	C-H stretching vibration of CH_3
1736	Valence vibration of C=O
1379	C-H bending vibration of CH_3
1250	C-O vibration of O-acetyl groups
878 813	Mannose pyranosyl ring

Table 4 Glycosyl-linkage analysis of DOP, DOPa, and DOPb.

Peak number	Retention time (min)	Corresponding derivatives	Residue linkage	Peak area percentage (%) [a]		
				DOP	DOPa	DOPb
1	12.45	2,3,4,6-Me_4-Man*p*	T-Man*p*	5.55	5.26	6.34
2	18.85	2,3,6-Me_3-Man*p*	1,4-linked-Man*p*	73.60	76.25	74.20
3	20.51	2,3,6-Me_3-Glc*p*	1,4-linked-Glc*p*	12.43	11.82	12.40
4	22.26	2,6-Me_2-Man*p*	1,3,4-linked-Man*p*	2.46	2.33	2.07
5	24.45	3,6-Me_2-Man*p*	1,2,4-linked-Man*p*	2.00	1.77	2.29
6	25.14	2,3-Me_2-Man*p*	1,4,6-linked-Man*p*	3.79	2.57	2.70

[a] Calculated as a relative percentage of all derivatives present, based on the peak area.
[b] DOP, DOPa, and DOPb were the samples of water-extracted polysaccharide from *Dendrobium officinale*, its two fractions DOPa (eluted with ultrapure water) and DOPb (eluted with 0.01 M NaCl), respectively.